Available online at www.sciencedirect.com
SCIENCE DIRECT®
Catalysis Today 101 (2005) 23–30
CATALYSIS TODAY
www.elsevier.com/locate/cattod

Partial oxidation of methane to synthesis gas on $Pt/Ce_xZr_{1-x}O_2$ catalysts: the effect of the support reducibility and of the metal dispersion on the stability of the catalysts

Fabio B. Passos [a,1], Elaine R. de Oliveira [a], Lisiane V. Mattos [b], Fabio B. Noronha [b,*]

[a] *Departamento de Engenharia Química e Programa de Pós-Graduação em Química Orgânica, Universidade Federal Fluminense, Rua Passos da Pátria 156, Niterói, Brazil*
[b] *Instituto Nacional de Tecnologia (INT), Av. Venezuela 82, CEP 20081-312, Rio de Janeiro, Brazil*

Available online 24 March 2005

Abstract

Pt/CeO_2, Pt/ZrO_2 and $Pt/Ce_xZr_{1-x}O_2$ catalysts containing different ceria and zirconia contents were studied in order to evaluate the effect of the support reducibility and metal dispersion on the stability of the catalyst on partial oxidation of methane reaction. Temperature programmed reduction (TPR) and oxygen storage capacity (OSC) results allowed evaluating the reducibility and oxygen transfer capacity of the catalysts. Metal dispersion was determined through cyclohexane dehydrogenation, a structure insensitive reaction. $Pt/Ce_xZr_{1-x}O_2$ catalysts proved to be more active, stable and selective than Pt/CeO_2 and Pt/ZrO_2 catalysts. The results showed that the stability of these catalysts depends not only on the amount of oxygen vacancies of the support but also on the metal particle size. The higher reducibility and oxygen storage/release capacity of $Pt/Ce_xZr_{1-x}O_2$ catalysts promotes the mechanism of continuous removal of carbonaceous deposits from the active sites, which takes place at the metal-support interfacial perimeter. On the other hand, the increase of metal particle size decreases the metal-support interfacial area, reducing the effectiveness of the cleaning mechanism of metal particle.

Keywords: Partial oxidation of methane; $Pt/Ce_xZr_{1-x}O_2$ catalysts; Oxygen storage capacity; Metal dispersion; Synthesis gas production; Gas-to-liquids technology (GTL).

1. Introduction

The nowadays situation of natural gas market opens up an window of opportunity to convert natural gas to liquid hydrocarbon fuels, the so-called GTL process [1]. The classical GTL route encloses the formation of synthesis gas, followed by the Fischer–Tropsch synthesis. The economical viability of this process relies strongly on the decrease of the costs of synthesis gas generation. Catalytic partial oxidation of methane is an interesting alternative for the production of synthesis gas. It is a mildly exothermic reaction and it provides a H_2/CO ratio equal to 2 (Eq. (1)), which is suitable for the subsequent use in the Fischer–Tropsch synthesis [2–9].

$$CH_4 + 0.5O_2 \rightarrow CO + 2H_2, \quad \Delta H^0_{298K} = -35.6\,\text{kJ/mol} \tag{1}$$

One of the main problems in methane conversion is the formation of coke. One of the strategies that have been tested to circumvent this problem is to design catalysts with components able to store or release oxygen during reaction conditions. In this sense, several authors have tested the addition of CeO_2 to catalytic formulations [10,11]. Yan et al. [10] reported that the selectivity to synthesis gas increased with the CeO_2 content of $Pt/CeO_2/Al_2O_3$ catalysts. Fathi et al. [11] observed that the selectivity to syngas on partial

* Corresponding author. Tel.: +55 21 2123 1177; fax: +55 21 2123 1051.
E-mail addresses: fbpassos@engenharia.uff.br (F.B. Passos), fabiobel@int.gov.br (F.B. Noronha).
[1] Fax: 55 21 2717 4446.

0920-5861/$ – see front matter © 2004 Elsevier B.V. All rights reserved.
doi:10.1016/j.cattod.2004.12.006

oxidation of methane using $Pt/CeO_2/Al_2O_3$ and $Rh/CeO_2/Al_2O_3$ was improved when the reduction degree of the cerium oxide increased. According to these authors, methane activation occurs on the metal surface. Oxygen migrates from the cerium oxide to the metal surface through spillover, followed by cerium oxide reduction. On the other hand, the stability of Ni/CeO_2 catalysts on the partial oxidation of methane was dependent on the dispersion of Ni [12].

The incorporation of ZrO_2 into CeO_2 lattice promotes the CeO_2 redox properties. The presence of ZrO_2 strongly increases the oxygen vacancies of the support due to the high oxygen mobility of the solid solution formed [13,14]. Despite of the large use of $CeZrO_2$ as a promoter in the automotive three way catalysts (TWC), there is scarce information about the performance of $CeZrO_2$ supported metal catalysts on the partial oxidation of methane [15,16].

We have recently studied the performance of Pt/Al_2O_3, Pt/ZrO_2 and $Pt/Ce_{0.75}Zr_{0.25}O_2$ catalysts on partial oxidation of methane [15]. $Pt/Ce_{0.75}Zr_{0.25}O_2$ catalyst proved to be more active, stable and selective than Pt/Al_2O_3 and Pt/ZrO_2 catalysts. The results showed that the stability of this material on this reaction is due to the high oxygen storage capacity of the support. The higher amount of lattice oxygen near the metal particles promotes the mechanism of carbon removal from the metallic surface, which takes place at metal-support interfacial perimeter. TPSR experiments showed that the partial oxidation of methane proceeded through a two-step mechanism. First, combustion of methane takes place, producing CO_2 and H_2O, then, synthesis gas is produced via carbon dioxide and steam reforming reaction of unreacted methane.

Pantu et al. [16] performed the methane partial oxidation on $Pt/Ce_xZr_{1-x}O_2$ catalysts ($x = 0.5$; 0.8; 1.0) in the absence of gaseous oxygen, using only lattice oxygen. The addition of zirconia to ceria significantly increased the methane oxidation rate and the reducibility of the cerium oxide but decreased the selectivity to carbon monoxide. They suggested that the oxidation of chemisorbed carbon at the metal-oxide perimeter or interface should not be the rate determining steps since metal dispersion was constant. They also ruled out the solid-state diffusion as a rate determining step due to the fast reoxidation of the reduced oxides observed in the oxygen pulse experiments. They concluded that further work was needed to sort out these issues. According to these authors, carbon deposition on metal particles can suppress the partial oxidation reaction before depletion of the available lattice oxygen at high methane concentration in the feed. Therefore, carbon deposition could be a problem in industrial application of this catalyst when the feed is pure methane. This result is completely different from the ones we have observed in our previous studies carried out under pure methane. In that case, $CeZrO_2$ supported catalysts were stable due to a clean mechanism derived from the redox properties of this support [15].

Then, in order to clarify these discrepancies, we further investigated the effect of the Ce/Zr ratio and the metal dispersion on the performance of $Pt/Ce_xZr_{1-x}O_2$ catalysts ($x = 0.00$; 0.25; 0.50; 0.75; 1.00) on the partial oxidation of methane. The catalysts were characterized by X-ray diffraction (XRD), temperature programmed reduction (TPR), oxygen storage capacity measurements (OSC) and cyclohexane dehydrogenation as a measure of exposed metal surface.

2. Experimental

2.1. Catalyst preparation

ZrO_2 support was prepared by calcination of zirconium hydroxide (MEL Chemicals) at 1073 K for 1 h in a muffle. CeO_2 support was obtained using a precipitation method through the addition of an excess of ammonium hydroxide to an aqueous solution of cerium(IV) ammonium nitrate. Then, the precipitate was washed with distilled water and calcined at 1073 K for 1 h in a muffle. Ce–ZrO_2 supports were synthesized following the method published by Hori et al. [17]. An aqueous solution of cerium(IV) ammonium nitrate and zirconium nitrate (Aldrich) was prepared with three different compositions: (i) 75 mol% CeO_2 and 25 mol% ZrO_2 ($Ce_{0.75}Zr_{0.25}O_2$); (ii) 50 mol% CeO_2 and 50 mol% ZrO_2 ($Ce_{0.50}Zr_{0.50}O_2$); and (iii) 25 mol% CeO_2 and 75 mol% ZrO_2 ($Ce_{0.25}Zr_{0.75}O_2$). Then, the ceria and zirconium hydroxides were co-precipitated by the addition of an excess of ammonium hydroxide. Finally, the precipitate was washed with distilled water and calcined at 1073 K for 1 h in a muffle. Furthermore, a CeO_2–ZrO_2 support with 14 mol% CeO_2 and 86 mol% ZrO_2 ($Ce_{0.14}Zr_{0.86}O_2$) supplied by MEL Chemicals was calcined at 1073 K for 1 h in a muffle. The catalysts were prepared by incipient wetness impregnation of the supports with an aqueous solution of H_2PtCl_6 (Aldrich) and were dried at 393 K. After impregnation, the samples were calcined under air (50 cm^3/min) at 673 K for 2 h. All samples contained 1.5 wt.% of platinum.

2.2. BET surface area

The BET surface areas of catalysts were measured using a Micromeritics ASAP 2000 analyzer by nitrogen adsorption at liquid nitrogen temperature.

2.3. X-ray diffraction

X-ray diffraction measurements were carried out using a RIGAKU diffractometer with a Cu Kα radiation. After calcination at 1073 K of supports, the XRD data were collected at 0.04°/step with integration times of 1 s/step. Crystallite sizes were estimated from the integral breadth of

the line with the higher intensity using the Scherrer equation [18].

2.4. Temperature programmed reduction

Temperature programmed reduction measurements were carried out in a micro-reactor coupled to a quadrupole mass spectrometer (Balzers, Omnistar). The samples (300 mg) were dehydrated at 423 K for 30 min in a He flow prior to reduction. After cooling to room temperature, a mixture of 5% H_2 in Ar flowed through the sample at 30 cm^3/min, raising the temperature at a heating rate of 10 K/min up to 1273 K.

2.5. Oxygen storage capacity

Oxygen storage capacity measurements were carried out in a micro-reactor coupled to a quadrupole mass spectrometer (Omnistar, Balzers). Prior to OSC analysis, the samples were reduced under H_2 at 773 K for 1 h and heated to 1073 K in flowing He. Then, the samples were cooled to 723 K and remained at this temperature during the analysis. The mass spectrometer was used to measure the composition of the reactor effluent as a function time, while a 5% O_2/He mixture was passed through the catalyst. Oxygen consumption was calculated from the curve corresponding to $m/e = 32$ taking into account a previous calibration of the equipment.

2.6. Cyclohexane dehydrogenation

Platinum dispersion was estimated through cyclohexane dehydrogenation, a structure insensitive reaction [19]. Since H_2 and CO adsorption occurs over CeO_2 and Ce–ZrO_2 supports, platinum dispersion could not be determined from chemisorption of both gases [20]. Then, in order to estimate the dispersion of Pt/ZrO_2, Pt/CeO_2 and Pt/Ce-ZrO_2 catalysts, a correlation between the rate of cyclohexane dehydrogenation and platinum dispersion measured by hydrogen chemisorption established for Pt/Al_2O_3 catalysts was employed. This methodology was used successfully before [21].

Cyclohexane dehydrogenation was performed in a fixed-bed reactor at atmospheric pressure. The catalysts were reduced at 773 K for 1 h and the reaction was carried out at 543 K and WHSV = 170 h^{-1}. The reactants were fed to the reactor by bubbling H_2 through a saturator containing cyclohexane at 285 K (H_2/HC = 13.6). The exit gases were analyzed using a gas chromatograph (HP5890) equipped with a HP-INNOWAX column.

2.7. Partial oxidation of methane

Partial oxidation of methane was performed in a quartz reactor (13 mm i.d.) at atmospheric pressure. Prior to reaction, the catalyst was reduced under H_2 at 773 K for 1 h and then heated to 1073 K under N_2. The reaction was carried out at 1073 K and WHSV = 520 h^{-1} over all catalysts. A reactant mixture with CH_4:O_2 ratio of 2:1 and a flow rate of 100 cm^3/min was used. In order to avoid temperature gradients, catalyst samples (20 mg) were diluted with inert SiC (36 mg) with the bed height being around 3 mm. The tranfer lines were kept at 413 K to avoid condensation. The exit gases were analysed using a gas chromatograph (Agilent 6890) equipped with a thermal conductivity detector and a CP-carboplot column (Chrompack).

3. Results and discussion

3.1. Characterization of the samples

Table 1 shows BET surface areas obtained for all catalysts. All catalysts exhibited low surface areas. The addition of Zr to ceria increased the surface area of the catalysts from 9 to 34–47 m^2/g, depending on composition. Terrible et al. [22] obtained similar values of surface area for Ce–ZrO_2 supports prepared by co-precipitation method. The enhancement of the surface area with the addition of zirconia to ceria was also observed by Hori et al. [17].

Fig. 1 shows the X-ray diffraction patterns of CeO_2 and ZrO_2 supports obtained after calcination at 1073 K. A cubic phase (JCPDS–4-0593) for CeO_2 and a monoclinic phase (JCPDS–13–307) for ZrO_2 support were observed. Noronha

Table 1
BET surface areas for all catalysts

Catalyst	BET surface area (m^2/g_{cat})
Pt/CeO_2	9
Pt/ZrO_2	20
Pt/$Ce_{0.75}Zr_{0.25}O_2$	34
Pt/$Ce_{0.50}Zr_{0.50}O_2$	43
Pt/$Ce_{0.25}Zr_{0.75}O_2$	47
Pt/$Ce_{0.14}Zr_{0.86}O_2$	43

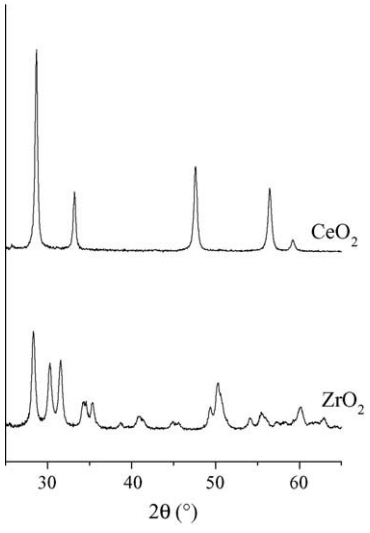

Fig. 1. X-ray diffraction patterns of CeO_2 and ZrO_2 supports.

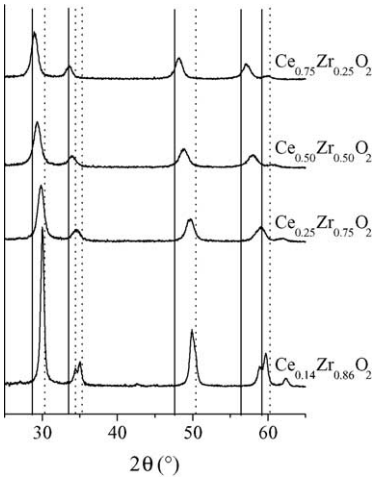

Fig. 2. X-ray diffraction patterns of $Ce_{0.75}Zr_{0.25}O_2$, $Ce_{0.50}Zr_{0.50}O_2$, $Ce_{0.25}Zr_{0.75}O_2$ and $Ce_{0.14}Zr_{0.86}O_2$ supports. The solid vertical lines are characteristic of cubic ceria and the broken vertical lines are characteristic of tetragonal zirconia.

et al. [23] reported the same result for a Pt/ZrO_2 catalyst calcined at 1073 K.

The X-ray diffraction patterns of $Ce_{0.75}Zr_{0.25}O_2$, $Ce_{0.50}Zr_{0.50}O_2$, $Ce_{0.25}Zr_{0.75}O_2$ and $Ce_{0.14}Zr_{0.86}O_2$ supports are presented in Fig. 2. The addition of 25% of ZrO_2 to CeO_2 did not result in a separate zirconia phase. However, the ceria peaks shifted from $2\theta = 28.6^\circ$ to $2\theta = 29.0^\circ$ and from $2\theta = 33.2^\circ$ to $2\theta = 33.5^\circ$. Hori et al. [17] studied the effect of ZrO_2 addition to CeO_2 on the phase composition of $Pt/CeZrO_2$ catalysts, using XRD experiments. Their discussion was based on the peaks at $2\theta = 28.6^\circ$ and 33.1° for cubic CeO_2. They also observed that the ceria peaks shift from $2\theta = 28.6^\circ$ to $2\theta = 29.0^\circ$ and from $2\theta = 33.1^\circ$ to $2\theta = 33.5^\circ$ by adding 25% of ZrO_2 to CeO_2. According to these authors, this shift is related to the formation of a CeO_2–ZrO_2 solid solution with a cubic symmetry. Noronha et al. [23] also obtained a cubic Ce–Zr solid solution for $Pt/Ce_{0.75}Zr_{0.25}O_2$ catalyst calcined at 1073 K.

By adding 50% of ZrO_2, a shift of ceria peaks from $2\theta = 28.6^\circ$ to $2\theta = 29.3^\circ$ and from $2\theta = 33.1^\circ$ to $2\theta = 33.8^\circ$ was observed. Similar results were obtained by Hori et al. [17] and Fornasiero et al. [24] for $Ce_{0.50}Zr_{0.50}O_2$ support. These results indicate that a single phase (Zr doped cubic ceria) was formed, but a small amount of a different phase (Ce doped tetragonal Zr) could be present [17].

When 75% of ZrO_2 was added, no separate zirconia phase was detected. In addition, the presence of peaks at $2\theta = 29.8^\circ$ and $2\theta = 34.5^\circ$ was observed. According to the literature [25], these results suggest the formation of a solid solution with tetragonal symmetric for $Ce_{0.25}Zr_{0.75}O_2$ support.

For $Ce_{0.14}Zr_{0.86}O_2$ support, the peak at $2\theta = 30.0^\circ$ overlaps with a zirconia line at $2\theta = 30.1^\circ$, while the doublet at $2\theta = 34.4^\circ$ and 35.0° is close to the tetragonal zirconia line (peaks at $\sim 2\theta = 34.5^\circ$ and 35.3°) shifted to small angles due to the presence of small amount of Ce^{4+} in the zirconia lattice. Similar results were obtained by Hori et al. [17] for $Ce_{0.25}Zr_{0.75}O_2$ support and suggest the formation of a tetragonal zirconia phase and a tetragonal Ce–Zr solid solution.

Table 2
The particle size determined by XRD experiments

Sample	Particle size (nm)
CeO_2	26
$Ce_{0.75}Zr_{0.25}O_2$	9
$Ce_{0.50}Zr_{0.50}O_2$	8
$Ce_{0.25}Zr_{0.75}O_2$	9
$Ce_{0.14}Zr_{0.86}O_2$	15

Table 2 shows the particle size determined by XRD for CeO_2, $Ce_{0.75}Zr_{0.25}O_2$, $Ce_{0.50}Zr_{0.50}O_2$, $Ce_{0.25}Zr_{0.75}O_2$ and $Ce_{0.14}Zr_{0.86}O_2$ supports. The addition of ZrO_2 to CeO_2 caused a decrease of particle size. Several authors have reported similar results for CeO_2–ZrO_2 systems [17,26]. According to the literature [26], the use of ZrO_2 improves the thermal stability of CeO_2, avoiding the sintering process.

Among the Ce–ZrO_2 supports, $Ce_{0.14}Zr_{0.86}O_2$ support showed the highest particle size. This result can be attributed to the formation of a non-homogeneous solid solution on $Ce_{0.14}Zr_{0.86}O_2$ support, as described above. Several authors [17,26] observed that a non-homogeneous solid solution could be responsible for the particle agglomeration. Furthermore, for $Ce_{0.75}Zr_{0.25}O_2$, $Ce_{0.50}Zr_{0.50}O_2$, $Ce_{0.25}Zr_{0.75}O_2$ supports, a similar particle size (about 8 nm) was obtained. Since these materials were prepared by the same method (co-precipitation), this result indicates that the composition of the solid solution have not affected the particle size.

The dispersion of the catalysts calculated through cyclohexane dehydrogenation is listed in Table 3. The dispersion increased in the order: $Pt/CeO_2 \sim Pt/Ce_{0.50}Zr_{0.50}O_2 < Pt/Ce_{0.75}Zr_{0.25}O_2 < Pt/ZrO_2 \sim Pt/Ce_{0.25}Zr_{0.75}O_2 \sim Pt/Ce_{0.14}Zr_{0.86}O_2$ catalyst.

3.2. Reduction behavior and oxygen storage capacity

The TPR profiles of CeO_2, ZrO_2, $Ce_{0.75}Zr_{0.25}O_2$, $Ce_{0.50}Zr_{0.50}O_2$, $Ce_{0.25}Zr_{0.75}O_2$ and $Ce_{0.14}Zr_{0.86}O_2$ supports are shown in Fig. 3.

Table 3
Specific rates of cyclohexane dehydrogenation and estimated platinum dispersion

Catalyst	Rate of cyclohexane dehydrogenation (mol/g_{cat} h)	Dispersion (%)
Pt/CeO_2	0.062	15
Pt/ZrO_2	0.116	29
$Pt/Ce_{0.75}Zr_{0.25}O_2$	0.090	22
$Pt/Ce_{0.50}Zr_{0.50}O_2$	0.056	14
$Pt/Ce_{0.25}Zr_{0.75}O_2$	0.119	30
$Pt/Ce_{0.14}Zr_{0.86}O_2$	0.135	34

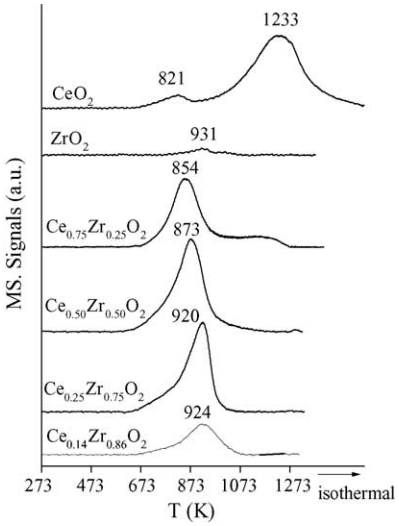

Fig. 3. Temperature programmed reduction profiles of CeO_2, ZrO_2, $Ce_{0.75}Zr_{0.25}O_2$, $Ce_{0.50}Zr_{0.50}O_2$, $Ce_{0.25}Zr_{0.75}O_2$ and $Ce_{0.14}Zr_{0.86}O_2$ supports.

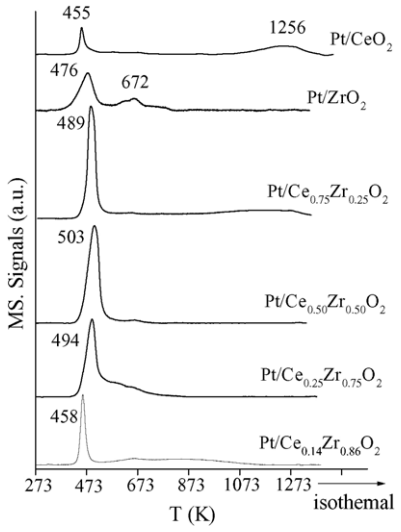

Fig. 4. Temperature programmed reduction profiles of Pt/CeO_2, Pt/ZrO_2, $Pt/Ce_{0.75}Zr_{0.25}O_2$, $Pt/Ce_{0.50}Zr_{0.50}O_2$, $Pt/Ce_{0.25}Zr_{0.75}O_2$ and $Pt/Ce_{0.14}Zr_{0.86}O_2$ catalysts.

For the CeO_2 support, a small H_2 uptake at 821 K and a strong H_2 consumption at 1233 K were observed. This result agrees with those reported by many authors [24,26–30]. According to them, the first peak is attributed to the surface reduction of CeO_2 and the second one to the formation of Ce_2O_3.

The ZrO_2 support was practically irreducible, showing only a small H_2 consumption around 931 K. Bozo et al. [28] obtained similar results in TPR experiments for zirconia.

The $Ce_{0.75}Zr_{0.25}O_2$, $Ce_{0.50}Zr_{0.50}O_2$, $Ce_{0.25}Zr_{0.75}O_2$ and $Ce_{0.14}Zr_{0.86}O_2$ supports presented a strong H_2 consumption at 854–924 K, which moved towards higher temperature as the zirconia content increased. Moreover, the $Ce_{0.75}Zr_{0.25}O_2$ support also showed a H_2 uptake around 1150 K. Fally et al. [27] studied the reducibility of CeO_2–ZrO_2 mixed oxides by TPR experiments. They also observed a presence of a peak at 843–863 K and a shift of its maximum as Zr content was increased.

Several authors [27,28,31] also reported the presence of only one peak at low temperature region on the TPR profiles of Ce–ZrO_2 oxides. According to these authors, this H_2 uptake is much higher than that needed for the reduction of ceria capping oxygen. It implies that several layers of the mixed oxide contribute to this peak, suggesting that the addition of ZrO_2 promotes the reduction of the bulk ceria. This was attributed to an improvement of the oxygen anion mobility induced by the insertion of ZrO_2 into the CeO_2 lattice [26].

Fig. 4 shows the TPR profiles of the Pt/CeO_2, Pt/ZrO_2, $Pt/Ce_{0.75}Zr_{0.25}O_2$, $Pt/Ce_{0.50}Zr_{0.50}O_2$, $Pt/Ce_{0.25}Zr_{0.75}O_2$ and $Pt/Ce_{0.14}Zr_{0.86}$ catalysts. The Pt/ZrO_2 catalyst showed H_2 uptakes at 476 and 672 K. The first peak was related to PtO_2 reduction, according to stoichiometric calculation and the peak at 672 K was attributed to the support reduction. The TPR profile of the Pt/CeO_2 catalyst presented two peaks at 455 and 1256 K, respectively. The former corresponds not only to the PtO_2 reduction but also to CeO_2 surface reduction, since the H_2 uptake was higher than the one related of platinum oxide. The peak at 1256 K is ascribed to bulk CeO_2 reduction.

All Pt/Ce-ZrO_2 catalysts showed a TPR peak at around 458–503 K that may be attributed to the reduction of platinum oxide and to the reduction of mixed oxide catalyzed by platinum. On the $Pt/Ce_{0.75}Zr_{0.25}O_2$ catalyst, a small H_2 uptake was also observed above 950K and it is related to the partial reduction of the support. $Pt/Ce_{0.25}Zr_{0.75}O_2$ catalyst exhibited a shoulder at 600 K, whereas $Pt/Ce_{0.14}Zr_{0.86}O_2$ catalyst presented small hydrogen consumption at temperatures higher than 600 K. These hydrogen uptakes above 600 K are also due to the partial reduction of the support.

A comparison between the TPR profiles of supports and catalysts shows that the addition of Pt promotes the reduction of support. This promoting effect is due to the hydrogen spillover from metal particles onto the support [26].

Table 4 presents the oxygen uptakes measured for the catalysts. The Pt/ZrO_2 and Pt/CeO_2 catalysts exhibit low oxygen consumption. On the other hand, the oxygen storage capacity of the Pt/Ce-ZrO_2 catalysts is considerably higher

Table 4
O_2 uptakes measured at 723 K

Catalyst	O_2 uptake ($\mu mol/g_{catal}$)
Pt/CeO_2	18
Pt/ZrO_2	9
$Pt/Ce_{0.75}Zr_{0.25}O_2$	626
$Pt/Ce_{0.50}Zr_{0.50}O_2$	696
$Pt/Ce_{0.25}Zr_{0.75}O_2$	519
$Pt/Ce_{0.14}Zr_{0.86}O_2$	220

than the one of the Pt/ZrO_2 and Pt/CeO_2 catalysts. Furthermore, the increase of ZrO_2 molar content from 25 to 50% has not caused a significant change on OSC values. However, when the ZrO_2 molar content was increased to 75%, the oxygen uptake decreased.

The values of O_2 consumption obtained on $Pt/Ce\text{-}ZrO_2$ catalysts agree with those reported by Fally et al. [27] on CeO_2–ZrO_2 systems. The OSC values obtained for these mixed oxides with a zirconium content between 20 and 50% are very close. Fornasiero et al. [32] also obtained the maximum OSC values for intermediate ZrO_2 contents (25–50%).

Several studies [26,33] reported that cerium oxide has an oxygen exchange capacity, which is associated to the ability of cerium to act as an oxygen buffer by storing/releasing O_2 due to the Ce^{4+}/Ce^{3+} redox couple [33]. The incorporation of ZrO_2 into CeO_2 lattice promotes the CeO_2 redox properties. The presence of ZrO_2 strongly increases the oxygen vacancies of the support, increasing its reducibility. This result is very consistent with the TPR findings. The enhancement of oxygen vacancies is due to the high oxygen mobility of the solid solution formed, which was identified by our XRD data.

3.3. Partial oxidation of methane

Fig. 5 shows the methane conversion and H_2 selectivity versus time on stream (TOS) for all samples on partial oxidation of methane. The Pt/CeO_2 catalyst showed the lower initial activity on partial oxidation of methane, while the others samples presented similar initial conversion. Furthermore, the Pt/CeO_2, Pt/ZrO_2, $Pt/Ce_{0.50}Zr_{0.50}O_2$ and $Pt/Ce_{0.14}Zr_{0.86}O_2$ catalysts deactivated during the reaction.

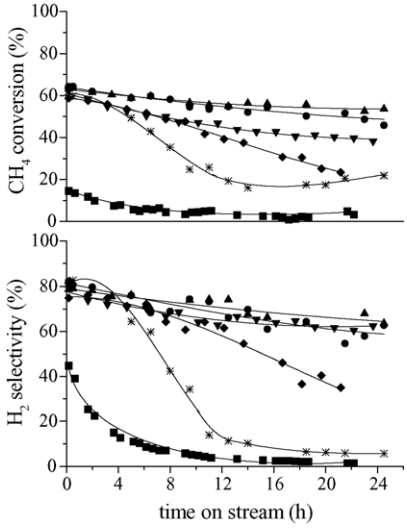

Fig. 5. Methane conversion and H_2 selectivity on partial oxidation of methane vs. time on stream for (■) Pt/CeO_2, (*) Pt/ZrO_2, (▲) $Pt/Ce_{0.75}Zr_{0.25}O_2$, (▼) $Pt/Ce_{0.50}Zr_{0.50}O_2$, (●) $Pt/Ce_{0.25}Zr_{0.75}O_2$ and (◆) $Pt/Ce_{0.14}Zr_{0.86}O_2$ catalysts. Reaction conditions: $T = 1073$ K; $CH_4{:}O_2$ ratio = 2:1.

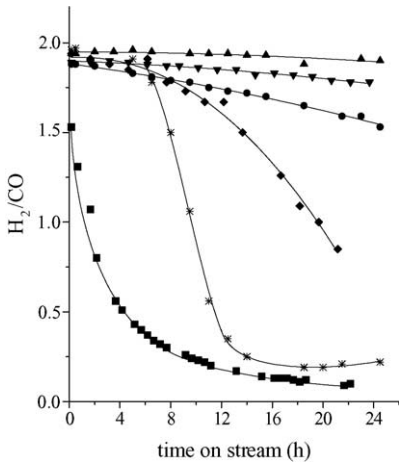

Fig. 6. H_2/CO ratio obtained from partial oxidation of methane vs. time on stream for (■) Pt/CeO_2, (*) Pt/ZrO_2, (▲) $Pt/Ce_{0.75}Zr_{0.25}O_2$, (▼) $Pt/Ce_{0.50}Zr_{0.50}O_2$, (●) $Pt/Ce_{0.25}Zr_{0.75}O_2$ and (◆) $Pt/Ce_{0.14}Zr_{0.86}O_2$ catalysts. Reaction conditions: $T = 1073$ K; $CH_4{:}O_2$ ratio = 2:1.

The $Pt/Ce_{0.75}Zr_{0.25}O_2$ and $Pt/Ce_{0.25}Zr_{0.75}O_2$ catalysts practically did not loose their activity after 24 h TOS.

The H_2 selectivity strongly decreased during the reaction for Pt/CeO_2, Pt/ZrO_2 and $Pt/Ce_{0.14}Zr_{0.86}O_2$ catalysts whereas it remained practically unchanged for $Pt/Ce_{0.75}Zr_{0.25}O_2$, $Pt/Ce_{0.50}Zr_{0.50}O_2$ and $Pt/Ce_{0.25}Zr_{0.75}O_2$ catalysts.

For $Pt/Ce_{0.50}Zr_{0.50}O_2$ and $Pt/Ce_{0.75}Zr_{0.25}O_2$ catalysts, the H_2/CO ratio obtained was approximately constant, whereas it decreased during the reaction for the other samples (Fig. 6). Moreover, the H_2/CO ratio was around two for $Pt/Ce_{0.75}Zr_{0.25}O_2$ catalyst and was lower than two for the other samples (Fig. 6). The values of H_2/CO ratio lower than two could be explained by the contribution of the reverse water

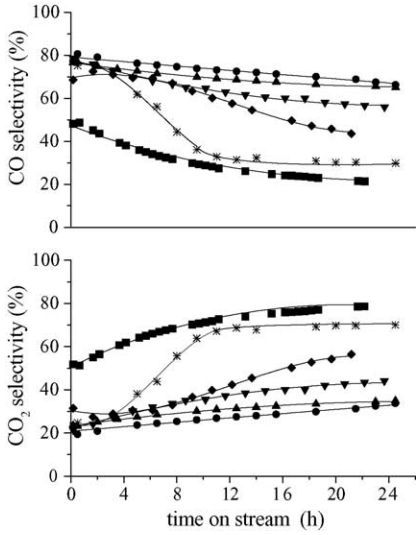

Fig. 7. CO and CO_2 selectivity on partial oxidation of methane vs. time on stream for: (■) Pt/CeO_2, (*) Pt/ZrO_2, (▲) $Pt/Ce_{0.75}Zr_{0.25}O_2$, (▼) $Pt/Ce_{0.50}Zr_{0.50}O_2$, (●) $Pt/Ce_{0.25}Zr_{0.75}O_2$ and (◆) $Pt/Ce_{0.14}Zr_{0.86}O_2$ catalysts. Reaction conditions: $T = 1073$ K; $CH_4{:}O_2$ ratio = 2:1.

gas shift reaction, which converts H_2 and CO_2 to CO and water [15,34].

The CO and CO_2 selectivities on partial oxidation of methane for all catalysts are presented in Fig. 7. The CO and CO_2 selectivity practically did not change during the reaction on $Pt/Ce_{0.75}Zr_{0.25}O_2$, $Pt/Ce_{0.50}Zr_{0.50}O_2$ and $Pt/Ce_{0.25}Zr_{0.75}O_2$ catalysts. On the other hand, on Pt/CeO_2, Pt/ZrO_2 and $Pt/Ce_{0.14}Zr_{0.86}O_2$ catalysts, the CO formation strongly decreased, while the production of CO_2 increased during TOS.

In the literature, the loss of activity of catalysts with time on stream on partial oxidation of methane has been attributed to carbon deposition [6,35–37]. Carbon formation has been characterized through different techniques such as thermogravimetric analysis [35,37], X-ray photoelectron spectroscopy [6] and transmission electron microscopy [36,37].

Recently, we have investigated the carbon formation and the capacity to remove carbon of the Pt/Al_2O_3, Pt/ZrO_2 and $Pt/Ce_{0.75}Zr_{0.25}O_2$ catalysts surface by using sequences of pulses of $CH_4/O_2/CH_4$ [15]. During the first set of CH_4 pulses, the conversion of methane decreased as the number of pulses increased, which was attributed to coke deposition. During O_2 pulses, no H_2 was produced. CO and CO_2 were formed during the first O_2 pulses. This result evidenced the carbon formation on catalyst surface. In the second set of CH_4 pulses, the role of support on the removal of carbon was evidenced. During this set of CH_4 pulses, the CH_4 consumption, the H_2 production and the CO formation slightly decreased in comparison to the results obtained in the first set of CH_4 pulses on $Pt/Ce_{0.75}Zr_{0.25}O_2$ catalyst. On the other hand, a significant decrease in the CH_4 consumption, the H_2 production and the CO formation was observed on Pt/ZrO_2 and Pt/Al_2O_3 catalysts. These results indicated that the oxygen vacancies of $Ce_{0.75}Zr_{0.25}O_2$ support, formed during the first set of CH_4 pulses, were partially replenished during O_2 pulses and kept the metal surface free of carbon deposits.

We have studied the effect of the support on CO_2 reforming and partial oxidation of methane under severely deactivating conditions [38]. A strong deactivation and a significant change in the CO and CO_2 selectivities were observed for the Pt/Al_2O_3 catalyst during the reaction. On the other hand, the $Pt/Ce_{0.75}Zr_{0.25}O_2$ catalyst was quite stable on both reactions. The results were explained by the oxygen storage capacity of the support. For Pt/Al_2O_3 catalyst, which did not exhibit OSC, the carbon deposition around or near the metal particle inhibited the CO_2 dissociation on CO_2 reforming of methane. This affects the partial oxidation of methane, which comprehends two steps: combustion of methane followed by CO_2 and steam reforming of unreacted methane. The higher oxygen storage capacity of $Pt/Ce_{0.75}Zr_{0.25}O_2$ catalyst kept the metal surface clean and promoted the stability of the catalyst.

In this work, the results of catalytic activity on partial oxidation of methane demonstrated that the support plays an important role on the deactivation mechanism.

$Pt/Ce_xZr_{1-x}O_2$ catalysts containing different ceria and zirconia contents were studied in order to evaluate the effect of Ce/Zr ratio on the stability of the catalyst on partial oxidation of methane reaction. The TPR and OSC results showed that the reducibility and oxygen transfer capacity was higher for $Pt/Ce_{0.75}Zr_{0.25}O_2$, $Pt/Ce_{0.50}Zr_{0.50}O_2$ and $Pt/Ce_{0.25}Zr_{0.75}O_2$ catalysts due to the solid solution formation, as revealed by XRD analysis. Then, the higher stability observed on these samples could be attributed to their higher oxygen transfer ability, which promotes the carbon removal of metal surface. For Pt/CeO_2, Pt/ZrO_2 and $Pt/Ce_{0.14}Zr_{0.86}O_2$ catalysts, the CO_2 dissociation was influenced by the increase of carbon deposits near the metal particle, affecting the methane conversion and consequently the CO_2 reforming step of the partial oxidation of methane. In the work of Pantu et al. [16], the strong deacti-vation observed on their $Pt/Ce_xZr_{1-x}O_2$ catalysts is probably due to the transient nature of their experiments. In the presence of gaseous oxygen, the support vacancies can be replenish, which keeps the redox mechanism working. Therefore, even under high methane concentration, carbon deposition can be suppressed through the available lattice oxygen.

However, comparing the performance of the $Pt/Ce_{0.75}Zr_{0.25}O_2$, $Pt/Ce_{0.50}Zr_{0.50}O_2$ and $Pt/Ce_{0.25}Zr_{0.75}O_2$ catalysts, it is clear that $Pt/Ce_{0.50}Zr_{0.50}O_2$ catalyst exhibited a slight deactivation during the reaction in spite of its high OSC value.

Recently, it was shown that CO_2 dissociation takes place at the metal-support interfacial perimeter [39]. Therefore, the increase of metal particle size decreases the metal-support interfacial area, which reduces the effectiveness of the cleaning mechanism of metal particle. This can explain the lower stability of the catalyst containing 50 mol% of ceria on the series of $Pt/Ce_xZr_{1-x}O_2$ catalysts. This catalyst has the lower dispersion among the $Pt/Ce_xZr_{1-x}O_2$ catalysts (Table 3). Then, not only the stability of the supported Pt catalysts depends on the amount of oxygen vacancies of the support but also the metal particle size.

On the other hand, $Pt/Ce_{0.75}Zr_{0.25}O_2$ and $Pt/Ce_{0.25}Zr_{0.75}O_2$ catalysts exhibit similar performance on partial oxidation of methane. As previously discussed, the redox mechanism of carbon removal involves the oxygen vacancies near the metal particles. Although the $Pt/Ce_{0.75}Zr_{0.25}O_2$ catalyst has a larger amount of oxygen vacancies than $Pt/Ce_{0.25}Zr_{0.75}O_2$ catalyst, its metallic dispersion is smaller. Therefore, the amount of oxygen available per metal-support interfacial area should be approximately the same on both catalysts. This could explain why these catalysts are quite stable during the reaction. Therefore, the stability of the catalysts on partial oxidation is associated to a proper balance between oxygen transfer ability of the support and metal dispersion.

In order to evaluate only the effect of the reducibility of the support on the stability of the catalysts, the performance of $Pt/Ce_{0.14}Zr_{0.86}O_2$ and $Pt/Ce_{0.25}Zr_{0.75}O_2$ catalysts should be compared, since these samples exhibit the same

dispersion. $Pt/Ce_{0.25}Zr_{0.75}O_2$ catalyst was stable and had a high OSC value whereas $Pt/Ce_{0.14}Zr_{0.86}O_2$ catalyst deactivated and presented a low OSC value. These results support the model proposed and evidences clearly the role of the reducibility of the support on the cleaning mechanism.

4. Conclusions

The results obtained on the partial oxidation of methane showed the important role of the support reducibility and of the metal dispersion on the stability of the supported platinum catalysts. $Pt/Ce_xZr_{1-x}O_2$ catalysts presented higher stability than Pt/CeO_2 and Pt/ZrO_2 catalysts. These results were attributed to a proper balance between oxygen transfer ability of the support and metal dispersion. The higher rate of oxygen transfer keeps the metal surface free of carbon. This mechanism of carbon removal takes place at the metal-support interfacial perimeter. Among $Pt/Ce_xZr_{1-x}O_2$ catalysts, the catalyst containing 50 mol% of ceria presented a slight deactivation during the reaction in spite of its high OSC value. The dispersion results obtained from cyclohexane dehydrogenation showed that $Pt/Ce_{0.5}Zr_{0.5}O_2$ catalyst exhibited a lower metal dispersion compared to other $Pt/Ce_xZr_{1-x}O_2$. Since the increase of metal particle size decreases the metal-support interfacial area, the effectiveness of the cleaning mechanism is reduced for low metal dispersion. This could explain why this catalyst is less stable during the reaction. Furthermore, $Pt/Ce_{0.75}Zr_{0.25}O_2$ and $Pt/Ce_{0.25}Zr_{0.75}O_2$ catalysts exhibit high stability and similar performance on partial oxidation of methane, which was assigned to the same amount of oxygen available per particle-support interfacial area on both catalysts.

Acknowledgements

The authors wish to acknowledge the financial support of the CNPq/CTPETRO (462530/00-0), FNDCT/CTPETRO/PETROBRAS (65.04.1600.13; 21.01.0257.00) program, PADCT-III and FAPERJ (E-26/150.126/2001).

References

[1] V.K. Venkataraman, H.D. Guthrie, R.A. Avellanet, D.J. Driscoll, Stud. Surf. Sci. Catal. 119 (1998) 913.
[2] P.D.F. Vernon, M.L.H. Green, A.K. Cheetham, A.T. Ashcroft, Catal. Lett. 6 (1990) 181.
[3] D.A. Hickman, L.D. Schmidt, Science 259 (1993) 343.
[4] D.A. Hickman, E.A. Haupfear, L.D. Schmidt, Catal. Lett. 17 (1993) 223.
[5] D.A. Hickman, L.D. Schmidt, J. Catal. 138 (1992) 267.
[6] D. Dissanayake, M.P. Rosynek, K.C.C. Kharas, J.H. Lunsford, J. Catal. 132 (1991) 117.
[7] P.M. Torniainen, X. Chu, L.D. Schmidt, J. Catal. 146 (1994) 1.
[8] A.K. Bhattacharya, J.A. Breach, S. Chand, D.K. Ghorai, A. Hartridge, J. Keary, K.K. Mallick, Appl. Catal. A 80 (1992) L1.
[9] H. Dong, Z. Shao, G. Xiong, J. Tong, S. Sheng, W. Yang, Catal. Today 67 (2001) 3.
[10] Q. Yan, W. Chu, L. Gao, Z. Yu, S. Yuan, Stud. Surf. Sci. Catal. 119 (1998) 855.
[11] M. Fathi, E. Bjorgum, T. Viig, O.A. Rokstad, Catal. Today 63 (2000) 489.
[12] T. Zhu, M. Flytzani-Stephanopoulos, Appl. Catal. A 208 (2001) 403.
[13] P. Fornasiero, R. di Monte, G.R. Rao, J. Kaspar, S. Meriani, A. Trovarelli, M. Graziani, J. Catal. 151 (1995) 168.
[14] G. Vlaic, P. Fornasiero, S. Geremia, J. Kaspar, M. Graziani, J. Catal. 168 (1997) 386.
[15] L.V. Mattos, E.R. de Oliveira, P.D. Resende, F.B. Noronha, F.B. Passos, Catal. Today 77 (2002) 245.
[16] P. Pantu, K. Kim, G.R. Gavalas, Appl. Catal. A: Gen. 193 (2000) 203.
[17] C.E. Hori, H. Permana, K.Y. Ng Simon, A. Brenner, K. More, K.M. Rahmoeller, D. Belton, Appl. Catal. B 16 (1998) 105.
[18] F.B. Noronha, M. Schmal, R. Fréty, G. Bergeret, B. Moraweck, J. Catal. 186 (1999) 20.
[19] M. Boudart, Adv. Catal. 20 (1969) 153.
[20] P. Pantu, G.R. Gavalas, Appl. Catal. A 223 (2002) 253.
[21] F.B. Passos, R. Fréty, M. Schmal, Catal. Lett. 29 (1994) 109.
[22] D. Terribile, A. Trovarelli, J. Llorca, C. de Leitenburg, G. Dolcetti, Catal. Today 43 (1998) 79.
[23] F.B. Noronha, G. Fendley, R.R. Soares, W.E. Alvarez, D.E. Resasco, Chem. Eng. J. 11 (2001) 3775.
[24] P. Fornasiero, G. Balducci, R. Di Monte, J. Kaspar, V. Sergo, G. Gubitosa, A. Ferrero, M. Graziani, J. Catal. 164 (1996) 173.
[25] M. Yashima, H. Arashi, M. Kakihana, M. Yoshimura, J. Am. Ceram. Soc. 77 (1994) 1067.
[26] J. Kaspar, P. Fornasiero, M. Graziani, Catal. Today 50 (1999) 285.
[27] F. Fally, V. Perrichon, H. Vidal, J. Kaspar, G. Blanco, J.M. Pintado, S. Bernal, G. Colon, M. Daturi, J.C. Lavalley, Catal. Today 59 (2000) 373.
[28] C. Bozo, N. Guilhaume, E. Garbowski, M. Primet, Catal. Today 59 (2000) 33.
[29] C. de Leitenburg, A. Trovarelli, J. Llorca, F. Cavani, G. Bini, Appl. Catal. A 139 (1996) 161.
[30] R.S. Monteiro, F.B. Noronha, L.C. Dieguez, M. Schmal, Appl. Catal. A 131 (1995) 89.
[31] H. Vidal, J. Kaspar, M. Pijolat, G. Colon, S. Bernal, A. Cordón, V. Perrichon, F. Fally, Appl. Catal. B 27 (2000) 49.
[32] P. Fornasiero, R. Di Monte, G.R. Rao, J. Kaspar, S. Meriani, A. Trovarelli, M. Graziani, J. Catal. 151 (1995) 168.
[33] M.H. Yao, R.J. Baird, F.W. Kunz, T.E. Hoost, J. Catal. 166 (1997) 67.
[34] M.C.J. Bradford, M.A. Vannice, Appl. Catal. A: Gen. 142 (1996) 97.
[35] A.M. O'Connor, J.R.H. Ross, Catal. Today 46 (1998) 203.
[36] T. Takeguchi, S. Furukawa, M. Inoue, J. Catal. 202 (2001) 14.
[37] M.M.V.M. Souza, M. Schmal, Appl. Catal. A: Gen. 255 (2003) 83.
[38] L.V. Mattos, E.R. de Oliveira, D.E. Resasco, F.B. Passos, F.B. Noronha, Fuel Process. Technol. 83 (2003) 147.
[39] S.M. Stagg-Willians, F.B. Noronha, G. Fendley, D.E. Resasco, J. Catal. 194 (2000) 240.